Polyhedron 27 (2008) 2710–2720

Contents lists available at ScienceDirect

Polyhedron

journal homepage: www.elsevier.com/locate/poly

Preparation and *cis*-to-*trans* transformation study of square-planar $[Pt(L_n)_2Cl_2]$ complexes bearing cytokinins derived from 6-benzylaminopurine (L_n) by view of NMR spectroscopy and X-ray crystallography

Lucie Szüčová [a], Zdeněk Trávníček [a,*], Igor Popa [a,b], Jaromír Marek [a,c]

[a] Department of Inorganic Chemistry, Faculty of Science, Palacký University, CZ-771 47 Olomouc, Czech Republic
[b] Laboratory of Growth Regulators, Palacký University and Institute of Experimental Botany AS CR, CZ-783 71 Olomouc, Czech Republic
[c] Institute of Experimental Biology, Faculty of Science, Masaryk University, CZ-625 00 Brno, Czech Republic

ARTICLE INFO

Article history:
Received 8 April 2008
Accepted 20 May 2008
Available online 24 June 2008

Keywords:
Pt(II) complexes
Cytokinins
NMR spectroscopy
X-ray structures
In vitro cytotoxicity

ABSTRACT

Mononuclear, square-planar platinum(II) complexes involving derivatives of aromatic cytokinins as the ligands, and having the general formula *cis*-$[Pt(L_n)_2Cl_2]$ (**1–3**) and *trans*-$[Pt(L_n)_2Cl_2]$ (**4–6**), where $n = 1–3$, L_1 = 2-chloro-6-(benzylamino)-9-isopropylpurine, L_2 = 2-chloro-6-[(4-methoxybenzyl)amino]-9-isopropylpurine and L_3 = 2-chloro-6-[(2-methoxybenzyl)-amino]-9-isopropylpurine, have been synthesized and characterized by elemental analysis, MALDI-TOF mass, FT IR, ^1H, ^{13}C, ^{15}N and ^{195}Pt NMR spectral measurements. Dynamic *cis*-to-*trans* isomerization process of complex **1** in *N*,*N*′-dimethylformamide (DMF) has been investigated by means of multinuclear NMR spectroscopy. The solid-state structures of **1, 4** · $(DMF)_2$, and **5** have been determined by single crystal X-ray analysis. X-ray structures revealed that the heterocyclic ligands are coordinated to platinum *via* nitrogen atom N(7) in all the complexes studied. *In vitro* cytotoxicity of the prepared complexes against MCF7, G361, K562, and HOS has been evaluated. Owing to low solubility of the complexes in water, the cytotoxicity has been only tested up to 5 μM concentration. Unfortunately, all complexes have been found to be non-cytotoxic in the accessible concentration range.

1. Introduction

Nowadays, there is indisputable fact that a platinum drug called *Cisplatin*, i.e. *cis*-diamminedichloridoplatinum(II), of which the cytotoxic effects were discovered by Rosenberg et al. in the 1960s [1], and some its derivatives, represent a unique class of antineoplastic drugs used in current chemotherapy [2,3]. A high number of recently prepared *cis* and/or *trans*-$[Pt(L)_2Cl_2]$ (L = amine) complexes showed the possibility to inhibit cell division and growth of cancer cells [4]. This attribute initiated a great interest in the potential application of these inorganic substances in the treatment of tumors [4]. At present, novel potential platinum-based anticancer agents are still intensively studied with the intention to improve their therapeutic profiles to overcome their side effects and acquired resistance to the drugs [5,6]. Thus, an identification of *cis*/*trans* isomers was found to play a crucial role in the characterization of the above mentioned types of Pt(II) complexes because *cis* and *trans* isomers were found to possess substantially different cytotoxic effects when tested against various cancer cell lines [7]. This fact gave rise the reason to study the stereochemistry and geometric isomerism of square-planar complexes of the type $[Pt(L)_2X_2]$ (where L = a monodentate *N*-donor ligand, X = halide) in solid state as well as in solution. Above all, *cis*-to-*trans* isomerization of square–planar Pt(II) complexes in solution is still a subject of great interest. The formation of the *trans* isomer in a process which was supposed to give the *cis* isomer gave impulse to focus on this phenomenon, especially if this effect was already observed and determined, e.g. for $[Pt(L)_2Cl_2]$ complexes with L = aniline, 2,5-dimethyl-aniline or *p*-toluidine [8], cyclobutylamine [9], cyclohexylamine [10], and cycloheptylamine [11], Moreover, *cis*-to-*trans* isomerization reactions of $[Pt(L)_2X_2]$ complexes, where X = Cl, Br or NO_3^-, and L = pyridine or pyrimidine [12,13], ketoxime [14], and pyridine [15], were also previously reported. Generally, it may be concluded that the situation regarding the isomerization process may be a bit complicated in a solution mainly because of the fact that *trans*-isomers may be formed unexpectedly during the synthetic pathway or re-crystallization of *cis*-isomers from some solvents [9,10]. For that reason, the monitoring of *cis*-isomer behavior in solution was showed to be very contributing. For instance, *cis* and *trans*-$[Pt(amine)_2I_2]$ complexes were studied using ^{195}Pt NMR spectrometry in DMF and their *cis*-to-*trans* isomerization was observed [16]. Similarly, the geometric isomers distribution in case of platinum(II) complexes of the type $[M(L)_2X_2]$, where M = Pt or Pd, L = *N*-benzoyl-*N*′-propylthiourea, X = Cl, Br or I, in chloroform was studied by ^{195}Pt and ^1H NMR

* Corresponding author. Tel.: +420 585634944; fax: +420 585634954.
E-mail address: zdenek.travnicek@upol.cz (Z. Trávníček).

0277-5387/$ - see front matter © 2008 Elsevier Ltd. All rights reserved.
doi:10.1016/j.poly.2008.05.021

spectrometry and their *cis*-to-*trans* isomerization process was also investigated [17].

Besides the above-mentioned publications regarding the *Cisplatin*-like complexes, there exists a great number of scientific papers concerning with the preparation, characterization and biological activity testing of *cis* and *trans* Pt-complexes as well as the papers describing the conditions and rules for their DNA binding. Among them, the following may be highlighted as examples, e.g. [18–21].

Based on these facts, we focused our attention on the preparation and characterization of isomerically pure Pt(II) complexes bearing derivatives of plant growth hormones called cytokinins as N-donor ligands and on their *cis*-to-*trans* isomerization processes in solutions. One group of cytokinins, i.e. a class of natural or artificial plant growth regulators discovered in the 1950s [22–24], is represented by compounds bearing a 6-benzylaminopurine moiety. Cytokinins play a very important role in plant growth and development, including the promotion of cell division, senescence and apical dominance regulation, and nutritional signals transmission [25–27]. Since the 1990s, some cytokinin derivatives based on 2,6,9-trisubstituted purine moiety have been extensively studied due to their activity in the regulation of the eukaryotic cell cycle, more specifically, due to their significant inhibition of cyclin-dependent kinases (CDKs) [28,29]. The CDKs are protein kinase enzymes playing a considerable role in regulation of the cell cycle [30]. Some of these CDK inhibitors, e.g. 2-[2-(hydroxyl-ethyl)amino]-6-benzylamino-9-methylpurine (*Olomoucine*), 2-[3-(hydroxypropyl)amino]-6-benzylamino-9-isopropylpurine (*Bohemine*), and 2-{[1-(hydroxylmethyl)-propyl]-amino}-6-benzylamino-9-isopropylpurine (*Roscovitine*, also named as seliciclib or CYC202) were also found effective against the proliferation of some human cancer cell lines both *in vitro* and *in vivo* [31,32]. The reason why we use derivatives of aromatic cytokinins and/or cyclin-dependent kinase inhibitors derived from 6-benzylaminopurine as the ligands for the preparation of transition metal complexes is that the cytotoxicity may be improved after the coordination of these organic molecules to a suitable transition metal ion, *e.g.* to Pt(II) and Pd(II) [33,34], Cu(II) [35], Zn(II) [36] or Co(II) [37], as we have found in the case of complexes prepared previously in our laboratory. Up to now, the dynamic *cis*-to-*trans* isomerization process of Pt(II) complexes involving the above-discussed organic molecules has not been investigated using NMR spectrometry yet. However, the *cis*-to-*trans* isomerization process was previously investigated in the case of Pd(II) complexes of the type $[Pd(L)_2Cl_2]$, where L = cytokinins derived from 6-benzyalminopurine [34].

In this paper, we describe the preparation of a series of isomerically pure *cis* and *trans*-Pt(II) complexes of the general formula *cis*-$[Pt(L_n)_2Cl_2]$ and *trans*-$[Pt(L_n)_2Cl_2]$, where $n = 1–3$, L_1 = 2-chloro-6-(benzylamino)-9-isopropylpurine (**1, 4**), L_2 = 2-chloro-6-[(4-methoxybenzyl)-amino]-9-isopropylpurine (**2, 5**), L_3 = 2-chloro-6-[(2-methoxybenzyl)amino]-9-isopropylpurine (**3, 6**). The complexes have been fully characterized by means of elemental analysis, MALDI-TOF, FT IR and multinuclear NMR spectra, and complexes **1**, **4** and **5** also by single crystal X-ray analysis. The complexes were also investigated for their cytotoxic effects *in vitro* against four human cancer cell lines: MCF7, K 562, G 361 and HOS. The *cis*-to-*trans* isomerization process of the complexes in DMFA solutions was studied by means of ^{1}H, ^{13}C, ^{15}N and ^{195}Pt NMR spectroscopy.

2. Experimental

2.1. Materials

$PtCl_2$ was used as received from Sigma–Aldrich Co. The organic ligands 2-chloro-6-benzylamino-9-isopropylpurine (L_1), 2-chloro-6-[(4-methoxybenzyl)amino]-9-isopropylpurine (L_2) and 2-chloro-6-[(2-methoxybenzyl)amino]-9-isopropylpurine (L_3) were prepared by methods described in the literature [34]. Schematic representations of all the ligands used in this study including atom numbering are depicted in Fig. 1. Organic solvents used for the syntheses were purchased from Lachema Co., while *N*,*N*′-dimethylformamide-d_7 (99.5%) used for NMR spectroscopy was purchased from Sigma–Aldrich Co.

2.2. Synthesis of the complexes

2.2.1. General procedure for the preparation of cis-$[Pt(L_n)_2Cl_2]$ (**1–3**), $L_n = L_1–L_3$

An appropriate ligand (1 mmol) was dissolved in chloroform (15 mL) and added to a mixture of $PtCl_2$ (0.09 g, 0.5 mmol) in the same solvent (10 mL). The reaction mixture was stirred at −18 °C for 15 days. Obtained yellow or light orange solutions were filtered and the filtrate let to stand at room temperature. Yellowish or dark

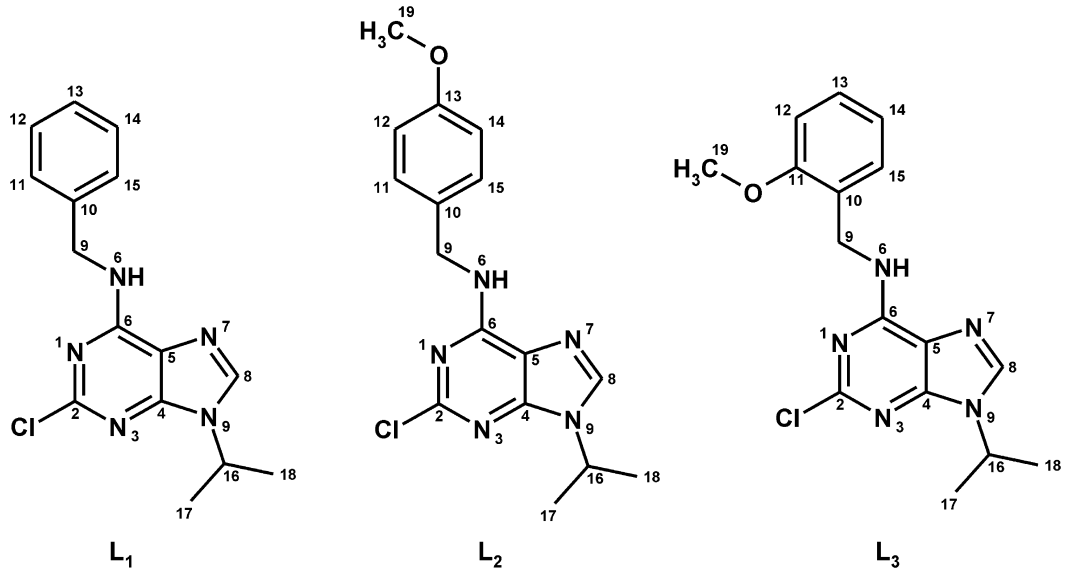

Fig. 1. A representation of organic molecules, including atom numbering scheme, used as ligands L_1–L_3.

yellow precipitates appeared after several days, which were filtered off, and dried in a vacuum desiccator over KOH.

*2.2.1.1. cis-[Pt(L$_1$)$_2$Cl$_2$] (**1**).* The complex was re-crystallized from chloroform and yellowish crystals suitable for X-ray crystallography were obtained by free evaporation of the solvent used. Yield: 76%. λ_M = 0.5 Ω cm^2 mol^{-1} in acetone, 0.8 Ω cm^2 mol^{-1} in DMF. FT-IR (KBr, cm^{-1}): 3342 (s, ν_{N-H}); 3092 (w, $\nu_{(C-H)ar}$); 1617 (vs, $\nu_{(C=N)ar}$), 1168 (m, $\nu_{(C-Cl)ar}$). FT-IR (Nujol, cm^{-1}): 348 (s, ν_{Pt-Cl}), 362 (vs, ν_{Pt-Cl}), 532 (vs, ν_{Pt-N}), 547 (s, ν_{Pt-N}). ^{1}H NMR (300 MHz, DMF-d_7, 300 K): δ 9.37 (1H, t, J = 6.0 Hz, N6H), δ 9.25 (1H, bs, C8H), δ 7.46 (2H, d, J = 7.3 Hz, C11,15H), δ 7.33 (2H, tt, J_a = 7.3 Hz, J_b = 1.5 Hz, C12,14H), δ 7.27 (1H, tt, J_a = 7.3 Hz, J_b = 1.5 Hz, C13H), δ 4.82 (1H, sep, J = 6.8 Hz, C16H), δ 4.90 (2H, s, C9H), δ 1.58 (6H, d, J = 6.8 Hz, C17,18H). ^{13}C NMR (75 MHz, DMF-d_7, 300 K): 155.10 (C6), 154.23 (C2), 149.88 (C4), 142.17 (C8), 139.32 (C10), 128.94 (C12,14), 127.84 (C11,15), 127.57 (C13), 116.37 (C5), 49.64 (C16), 45.02 (C9), 22.14 (C17,18). ^{15}N NMR (30 MHz, DMF-d_7, 340 K): 231.92 (N1), 184.54 (N9), 141.62 (N7), 99.05 (N6). ^{195}Pt (65 MHz, DMF-d_7, 300 K): −2017.88. MALDI-TOF-MS m/z: (positive mode) 906 (calc. for [M+K]$^+$), 906; 890.1 (calc. for [M+Na]$^+$) 890; 868.1 (calc. for [M+H]$^+$) 868; 833 (calc. for [{M−Cl}+H]$^+$) 833; 798 (calc. for [{M−2Cl}+H]$^+$) 798; 302 (calc. for [L+H]$^+$) 302. *Anal.* Calc. for $C_{30}H_{32}N_{10}Cl_4Pt$ (**1**): C, 41.4; H, 3.7; N, 16.1. Found: C, 41.5; H, 3.7; N, 15.9%.

*2.2.1.2. cis-[Pt(L$_2$)$_2$Cl$_2$] (**2**).* The complex was re-crystallized from chloroform. Yield: 70%. λ_M = 0.9 Ω cm^2 mol^{-1} in acetone, 2.0 Ω cm^2 mol^{-1} in DMF. FT-IR (KBr, cm^{-1}): 3316 (s, ν_{N-H}), 3103 (m, $\nu_{(C-H)ar}$); 1614 (vs, $\nu_{(C=N)ar}$), 1226 (s, ν_{Car-O}), 1033 (m, $\nu_{(C-O)alif}$), 1176 (m, $\nu_{(C-Cl)ar}$). FT-IR (Nujol, cm^{-1}): 340 (s, ν_{Pt-Cl}), 349 (m, ν_{Pt-Cl}), 521 (s, ν_{Pt-N}), 532 (s, ν_{Pt-N}). ^{1}H NMR (300 MHz, DMF-d_7, 300 K): δ 9.29 (1H, t, J = 6.1 Hz, N6H), δ 9.20 (1H, bs, C8H), δ 7.41 (2H, d, J = 8.6 Hz, C11,15H), δ 6.89 (2H, dd, J_a = 8.6 Hz, J_b = 2.2 Hz, C12,14H), δ 4.81 (1H, sep, J = 6.8 Hz, C16H), δ 4.82 (2H, s, C9H), 3.80 (3H, s, C19H), δ 1.57 (6H, d, J = 6.8 Hz, C17,18H). ^{13}C NMR (75 MHz, DMF-d_7, 300 K): 159.55 (C13), 155.10 (C6), 154.16 (C2), 149.84 (C4), 142.17 (C8), 131.00 (C10), 129.32 (C11,15), 116.38 (C5), 114.37 (C12,14), 55.51 (C19), 49.65 (C16), 44.55 (C9), 22.06 (C17,18). ^{15}N NMR (30 MHz, DMF-d_7, 340 K): 231.10 (N1), 184.47 (N9), 141.94 (N7), 100.70 (N6). ^{195}Pt (65 MHz, DMF-d_7, 300 K): −2017.36. MALDI-TOF-MS m/z: (positive mode) 966 (calc. for [M+K]$^+$), 966; 950.0 (calc. for [M+Na]$^+$) 950; 928 (calc. for [M+H]$^+$) 928; 893 (calc. for [{M−Cl}+H]$^+$) 893; 858 (calc. for [{M−2Cl}+H]$^+$) 858; 332 (calc. for [L+H]$^+$) 332. *Anal.* Calc. for $C_{32}H_{36}N_{10}O_2Cl_4Pt$ (**2**): C, 41.3; H, 3.9; N, 15.1. Found: C, 41.3; H, 3.9; N, 15.0%.

*2.2.1.3. cis-[Pt(L$_3$)$_2$Cl$_2$] (**3**).* The complex was re-crystallized from chloroform. Yield: 80%. λ_M = 1.5 Ω cm^2 mol^{-1} in acetone, 1.8 Ω cm^2 mol^{-1} in DMF. FT-IR (KBr, cm^{-1}): 3317 (s, ν_{N-H}), 3101 (w, $\nu_{(C-H)ar}$); 1620 (vs, $\nu_{(C=N)ar}$), 1243 (m, ν_{Car-O}), 1029 (m, $\nu_{(C-O)alif}$), 1163 (m, $\nu_{(C-Cl)ar}$). FT-IR (Nujol, cm^{-1}): 336 (s, ν_{Pt-Cl}), 345 (s, ν_{Pt-Cl}), 527 (s, ν_{Pt-N}), 549 (s, ν_{Pt-N}). ^{1}H NMR (300 MHz, DMF-d_7, 300 K): δ 9.32t (1H, t, J = 6.2 Hz, N6H), δ 9.15 (1H, bs, C8H), δ 7.38 (1H, bs, C15H), δ 7.29 (1H, t, J = 7.9 Hz, C13H), δ 7.06 (1H, d, J = 8.2 Hz, C12H), δ 6.86 (1H, t, J = 7.9 Hz, C14H), δ 4.79 (1H, sep, J = 6.8 Hz, C16H), δ 4.91 (2H, d, J = 6.0 Hz, C9H), δ 3.97 (3H, s, C19H), δ 1.55 (6H, d, J = 6.4 Hz, C17,18H). ^{13}C NMR (75 MHz, DMF-d_7, 300 K): 158.15 (C11), 155.12 (C6), 154.27 (C2), 149.79 (C4), 142.24 (C8), 129.17 (C13), 128.49 (C15), 126.42 (C10), 120.64 (C14), 116.37 (C5), 111.02 (C12), 56.05 (C19), 49.66 (C16), 40.90 (C9), 22.04 (C17,18). ^{15}N NMR (30 MHz, DMF-d_7, 340 K): 231.68 (N1), 184.50 (N9), 142.53 (N7), 98.32 (N6). ^{195}Pt (65 MHz, DMF-d_7, 300 K): −2023.06. MALDI-TOF-MS m/z: (positive mode) 966 (calc. for [M+K]$^+$), 966; 950.0 (calc. for [M+Na]$^+$) 950; 928 (calc. for [M+H]$^+$) 928; 332 (calc. for [L+H]$^+$) 332. *Anal.* Calc. for $C_{32}H_{36}N_{10}O_2Cl_4Pt$: C, 41.3; H, 3.9; N, 15.1. Found: C, 41.0; H, 3.9; N, 15.2%.

*2.2.2. General procedure for the preparation of trans-[Pt(L$_n$)$_2$Cl$_2$] (**4–6**), L$_n$ = L$_1$–L$_3$*

0.5 mmol of each of the *cis*-Pt isomers (**1**–**3**) was dissolved in DMF (10 mL). The solution was heated up to 50 °C and stirred for 15 min. Then, the solution was filtered and let to crystallize at the room temperature. The crystals of the complexes, in the case of **4** suitable for X-ray analysis, were obtained after 21 days.

*2.2.2.1. trans-[Pt(L$_1$)$_2$Cl$_2$] (**4**).* Dark yellow crystals suitable for X-ray crystallography were obtained by slow evaporation of the solvent. Yield: 50%. λ_M = 0.9 Ω cm^2 mol^{-1} in acetone, 2.4 Ω cm^2 mol^{-1} in DMF. FT-IR (KBr, cm^{-1}): 3331 (s, ν_{N-H}), 3110 (m, $\nu_{(C-H)ar}$); 1623 (vs, $\nu_{(C=N)ar}$), 1163 (m, $\nu_{(C-Cl)ar}$). FT-IR (Nujol, cm^{-1}): 348 (vs, ν_{Pt-Cl}), 542 (vs, ν_{Pt-N}). ^{1}H NMR (300 MHz, DMF-d_7, 300 K): δ 9.05 (1H, t, J = 6.0 Hz, N6H), δ 8.97 (1H, s, C8H), δ 7.56 (2H, dd, J_a = 7.3 Hz, J_b = 1.5 Hz, C11,15H), δ 7.35 (2H, tt, J_a = 7.3 Hz, J_b = 1.5 Hz, C12,14H), δ 7.28 (1H, tt, J_a = 7.3 Hz, J_b = 1.5 Hz, C13H), δ 4.95 (1H, sep, J = 6.8 Hz, C16H), δ 4.92 (2H, d, J = 6.2 Hz, C9H), δ 1.63 (6H, d, J = 6.8 Hz, C17,18H). ^{13}C NMR (75 MHz, DMF-d_7, 300 K): 155.15 (C6), 153.91 (C2), 149.60 (C4), 143.34 (C8), 138.77 (C10), 128.97 (C12,14), 128.05 (C11,15), 127.48 (C13), 115.99 (C5), 49.87 (C16), 45.24 (C9), 22.29 (C17,18). ^{15}N NMR (30 MHz, DMF-d_7, 340 K): 231.87 (N1), 224.80 (N3), 183.83 (N9), 133.20 (N7), 100.10 (N6). ^{195}Pt (65 MHz, DMF-d_7, 300 K): −2061.63. MALDI-TOF-MS m/z: (positive mode) 890.1 (calc. for [M+Na]$^+$) 890; 868 (calc. for [M+H]$^+$) 868; 833 (calc. for [{M−Cl}+H]$^+$) 833; 798 (calc. for [{M−2Cl}+H]$^+$) 798; 302 (calc. for [L+H]$^+$) 302. *Anal.* Calc. for $C_{30}H_{32}N_{10}Cl_4Pt$ (**4**): C, 41.4; H, 3.7; N, 16.1. Found: C, 41.5; H, 3.7; N, 16.0%.

*2.2.2.2. trans-[Pt(L$_2$)$_2$Cl$_2$] (**5**).* Orange crystals suitable for X-ray crystallography were obtained after slow evaporation of the solvent used. Yield: 65%. λ_M = 0.8 Ω cm^2 mol^{-1}. λ_M = 2.5 Ω cm^2 mol^{-1} in acetone, 3.2 Ω cm^2 mol^{-1} in DMF. FT-IR (KBr, cm^{-1}): 3300 (s, ν_{N-H}), 3120 (m, $\nu_{(C-H)ar}$); 1622 (vs, $\nu_{(C=N)ar}$), 1218 (s, ν_{Car-O}), 1028 (m, $\nu_{(C-O)alif}$), 1177 (m, $\nu_{(C-Cl)ar}$). FT-IR (Nujol, cm^{-1}): 347 (s, ν_{Pt-Cl}), 525 (s, ν_{Pt-N}). ^{1}H NMR (300 MHz, DMF-d_7, 300 K): δ 8.94 (1H, t, J = 6.0 Hz, N6H), δ 8.91 (1H, s, C8H), δ 7.49 (2H, dd, J_a = 8.6 Hz, J_b = 2.2 Hz, C11,15H), δ 6.90 (2H, dd, J_a = 8.6 Hz, J_b = 2.2 Hz, C12,14H), δ 4.94 (1H, sep, J = 6.8 Hz, C16H), δ 4.81 (2H, d, J = 6.06 Hz, C9H), 3.79 (3H, s, C19H), δ 1.64 (6H, d, J = 6.8 Hz, C17,18H). ^{13}C NMR (75 MHz, DMF-d_7, 300 K): 159.68 (C13), 155.28 (C6), 153.85 (C2), 149.60 (C4), 143.28 (C8), 130.45 (C10), 129.68 (C11,15), 116.06 (C5), 114.41 (C12,14), 55.51 (C19), 49.94 (C16), 44.95 (C9), 22.06 (C17,18). ^{15}N NMR (30 MHz, DMF-d_7, 340 K): 232.18 (N1), 224.68 (N3), 184.19 (N9), 133.66 (N7), 102.52 (N6). ^{195}Pt (65 MHz, DMF-d_7, 300 K): −2064.02. MALDI-TOF-MS m/z: (positive mode) 928 (calc. for [M+H]$^+$) 928; 893 (calc. for [{M−Cl}+H]$^+$) 893; 858 (calc. for [{M−2Cl}+H]$^+$) 858; 332 (calc. for [L+H]$^+$) 332. *Anal.* Calc. for $C_{32}H_{36}N_{10}O_2Cl_4Pt$ (**5**): C, 41.3; H, 3.9; N, 15.1. Found: C, 41.4; H, 3.8; N, 15.4%.

*2.2.2.3. trans-[Pt(L$_3$)$_2$Cl$_2$] (**6**).* Yield: 50%. λ_M = 0.9 Ω cm^2 mol^{-1} in acetone, 2.1 Ω cm^2 mol^{-1} in DMF. FT-IR (KBr, cm^{-1}): 3344 (s, ν_{N-H}), 3095 (w, $\nu_{(C-H)ar}$); 1619 (vs, $\nu_{(C=N)ar}$), 1244 (s, ν_{Car-O}), 1027 (m, $\nu_{(C-O)alif}$), 1166 (m, $\nu_{(C-Cl)ar}$). FT-IR (Nujol, cm^{-1}): 340 (s, ν_{Pt-Cl}), 530 (s, ν_{Pt-N}). ^{1}H NMR (300 MHz, DMF-d_7, 300 K): δ 9.00 (1H, t, J = 6.2 Hz, N6H), δ 9.02 (1H, s, C8H), δ 7.49 (1H, d, J = 7.9 Hz, C11,15H), δ 7.38 (1H, t, J = 7.9 Hz, C13H), δ 7.04 (1H, d, J = 8.2 Hz, C12H), δ 6.87 (1H, t, J = 7.9 Hz, C14H), δ 4.95 (1H, sep, J = 6.8 Hz, C16H), δ 4.88 (2H, d, J = 6.0 Hz, C9H), δ 3.82 (3H, s, C19H), δ 1.64 (6H, d, J = 6.8 Hz, C17,18H). ^{13}C NMR (75 MHz, DMF-d_7, 300 K):

158.03 (C11), 155.28 (C6), 154.13 (C2), 149.69 (C4), 143.37 (C8), 129.28 (C13), 128.62 (C15), 126.26 (C10), 120.73 (C14), 116.11 (C5), 111.02 (C12), 55.78 (C19), 49.88 (C16), 40.90 (C9), 22.04 (C17,18). ^{15}N NMR (30 MHz, DMF-d_7, 340 K): 231.76 (N1), 184.20 (N9), 133.98 (N7), 99.34 (N6). ^{195}Pt (65 MHz, DMF-d_7, 300 K): −2066.07. MALDI-TOF-MS *m*/*z*: (positive mode) 928 (calc. for $[M+H]^+$) 928; 893 (calc. for $[\{M-Cl\}+H]^+$) 893; 858 (calc. for $[\{M-2Cl\}+H]^+$) 858; 332 (calc. for $[L+H]^+$) 332. *Anal.* Calc. for $C_{32}H_{36}N_{10}O_2Cl_4Pt$ (**6**): C, 41.3; H, 3.9; N, 15.1. Found: C, 41.2; H, 4.0; N, 15.0%.

2.3. Physical measurements

Elemental analysis (C,H,N) was performed on the EA1112 Flash analyzer (ThermoFinnigan). Thin layer chromatography (TLC) of the prepared organic molecules was performed using a $CHCl_3$/CH_3OH/NH_4OH (8:2:0.1) mobile phase and carried out using Silica Gel 60 WF_{254} plates (Merck Co.). Positive ion MALDI-TOF mass spectra were measured in the reflection mode on a Microflex MALDI-TOF LRF20 mass spectrometer equipped with a nitrogen laser operating at 337 nm (Bruker Daltonik). MALDI-TOF-MS data of the studied complexes were measured acetone solutions (0.5 mM final concentration). Saturated solution of α-cyano-4-hydroxycinnamic acid in a 50%/0.2% acetonitrile/trifluoroacetic acid solution was used as a MALDI matrix. An aliquot of the sample solution in acetone (5 μL) and 5 μL of the matrix solution were premixed in a test tube. Then, 0.5 μL of the mixture was pipetted onto the target plate and allowed to dry at ambient temperature. Spectra were accumulated from 20 to 50 laser shots at a laser repetition rate of 10 Hz. The instrument was calibrated externally using a mixture of peptide standards. Acquired spectra were processed by FLEXANALYSIS 2.4 software (Bruker Daltonik). Post-source decay (PSD) spectra were recorded in 15 segments with each succeeding segment representing a 10% reduction in reflectron voltage. About 100 shots were averaged per segment. Segment spectra were pasted, calibrated and smoothed using the program FLEXANALYSIS 2.4. Conductivity measurements were performed on a Cond340i/SET conductometer (WTW, Germany) in DMF solution (10^{-3} M) at 25 °C. Far FT-IR spectra were measured using the Nujol technique in the range of 150–600 cm^{-1}, whilst mid FT-IR spectra were obtained by the KBr pellets technique between 400 and 4000 cm^{-1}, both using a NEXUS 670 FT-IR spectrometer (Thermo Nicolet). ^{1}H and ^{13}C NMR spectra were recorded on a Bruker Avance 300 spectrometer at 300 K. The samples were prepared by dissolving the ligands $\mathbf{L}_1$–$\mathbf{L}_3$ and complexes **1–6** in deuterated *N*,*N*′-dimethylformamide (DMF-d_7). The internal reference standard used for ^{1}H and ^{13}C NMR measurements was tetramethylsilane (TMS). ^{15}N NMR chemical shifts were measured relatively to the DMF-d_7 solvent (adjusted to 104.7 ppm). The individual ^{1}H and ^{13}C signals were assigned and refined by means of 2D correlation experiments of ^{1}H–^{1}H *gs*-COSY, ^{1}H–^{13}C *gs*-HMQC and ^{1}H–^{13}C *gs*-HMBC experiments. ^{15}N chemical shifts for the ligands $\mathbf{L}_1$–$\mathbf{L}_3$ and complexes **1–6** were obtained at natural abundance by ^{1}H–^{15}N *gs*-HMQC and ^{1}H–^{15}N *gs*-HMBC experiments and the spectra were recorded at 340 K.

2.4. X-ray crystallography

Diffraction data for single crystals of *cis*-Pt(II) complex of **1** and *trans*-Pt(II) complexes of **4** · $(DMF)_2$ and **5** were collected on an Xcalibur diffractometer (Oxford Diffraction) with Mo Kα (monochromator Enhance, Oxford Diffraction) radiation and ω-scan rotation techniques. The data were collected to maximum θ value of 25° and processed using the CRYSALIS software package (Oxford Diffraction, Ltd.) [38]. A multi-scan absorption correction integrated in the CRYSALIS software was applied on the data of all three complexes. All three structures were determined by direct methods using SHELXS-97 and refined anisotropically on F^2 using full-matrix least-squares procedure by SHELXL-97 [39]. H-atoms were positioned geometrically, with C–H distances of 0.95–1.00 Å and N–H distances of 0.88 Å, and with U_{iso}(H) values of 1.2U_{eq}(C,N). Most of atoms of the L_1 ligand in **1**, methyl groups of the isopropyl moiety in **4** · $(DMF)_2$, and all atoms of the isopropyl moiety as well as chlorine atom of the L_2 ligand in **5** were refined as disordered over two positions. Moreover, because of the disordered nature of the part of the structure in the case of **1**, isotropic restraints were placed on the anisotropic thermal parameters of some atoms of the L_1 ligand. All structural figures were made with DIAMOND [40].

2.5. Cytotoxicity testing

Cytotoxicity values of IC_{50} for complexes **1–6** and for the ligands L_1–L_3 were determined by a calcein AM assay. Human cancer cell lines *in vitro* were used as follows: malignant melanoma (G361), chronic myelogenous leukaemia (K562), osteogenic sarcoma (HOS), and breast adenocarcinoma (MCF7). The technique of the biological activity testing has been previously described in greater detail [33]. All the experiments were repeated in triplicate. The presented IC_{50} values are represented by arithmetic mean values, with a maximal deviation of 15%. All the ligands and complexes were first dissolved in DMF and then immediately diluted in water to a final DMF concentration of 0.6%.

3. Results and discussion

3.1. Synthetic aspects and conductivity measurement results

Scheme 1 illustrates the synthetic pathway that led to the preparation both L_n organic molecules, used as ligands, and *cis*-$[Pt(L_n)_2Cl_2]$ (**1–3**) and *trans*-$[Pt(L_n)_2Cl_2]$ (**4–6**) complexes. As the first step of the complex syntheses, *cis* isomers were prepared. Yellow to light orange solutions appeared after mixing the reactants at the temperature of −18 °C. Then, the reaction mixtures were filtered off in order to remove visible residues originating from initial $PtCl_2$ and let to stand at the temperature of −18 °C for next few days. Yellow precipitates, which appeared after this time period, were collected by filtration and re-crystallized from chloroform (**1–3**). *Trans* isomers were obtained after dissolving of the powdery samples of the appropriate *cis* isomers in DMF. The whole procedure was supported by heating up to 50 °C. Based on our next experiences, *trans* isomers could be also obtained by elongation of the reaction time by several weeks supported by heating (60–70 °C). Generally, it is known that a *cis-to-trans* isomerization process of square-planar Pt(II) complexes can be caused both by recrystallization of *cis* isomers from various solvents (e.g. acetone [9–11], DMF [41], $CHCl_3$ [17]) or solid state thermal heating [14].

All the complexes behave as non-electrolytes both in acetone and DMF solutions with the conductivity values found within the interval of 0.5–2.5 and 1.2–3.2 Ω cm^2 mol^{-1} in acetone, and DMF, respectively. The obtained conductivity values are consistent with the literature data obtained for other complex non-electrolytes [42].

3.2. Mass and FT IR spectral studies

The positive ion MALDI-TOF mass spectra were carried out for all complexes **1–6**. They showed molecular ion $[M+H]^+$ peaks in the spectra of complexes **1–3**, and moreover, the $[M+K]^+$ molecular adduct ions also appeared. Fig. 2 depicts the isotopic distribution of the molecular peak obtained for complex **1** compared to the calculated one obtained using the MASSLYNXTM software taking into

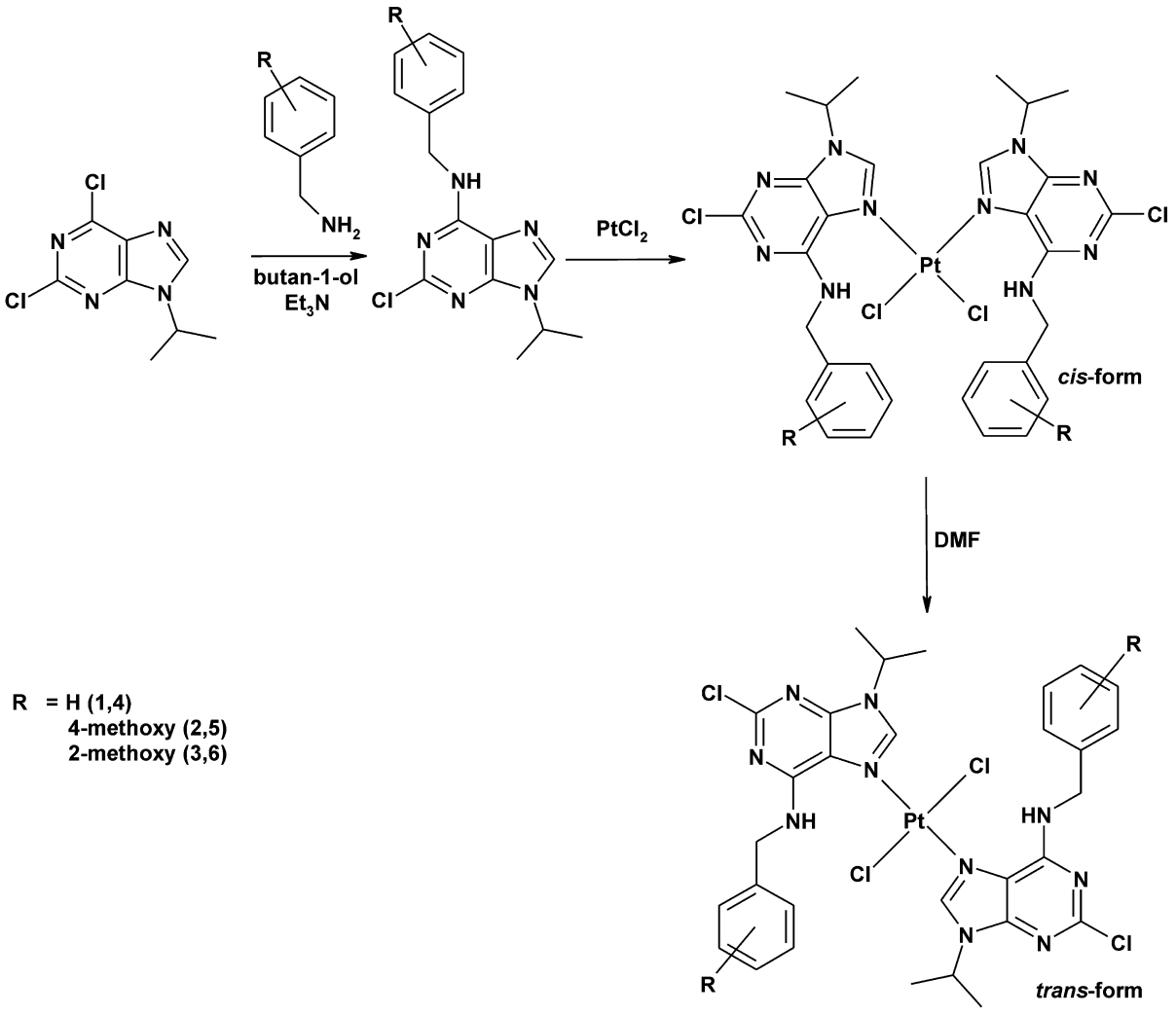

Scheme 1. Schematic representation of the synthesis of ligands and *cis* (**1**–**3**) and *trans* (**4**–**6**) Pt(II) complexes.

account the isotopic representation of all the atoms within the molecule [43]. For complexes **1–4**, there were also found $[M+Na]^+$ molecular adduct ions. Generally, the formation of adducts with Na^+ and K^+ is typical for this type of complexes [44]. All the complexes, except for **3**, showed at least two fragments, *i.e.* $[\{M-Cl\}+H]^+$ and $[\{M-2Cl\}+H]^+$. Moreover, the molecular peak of the appropriate ligand, $[L+H]^+$, appeared in all spectra of the complexes.

FT-IR spectra of both the ligands L_1–L_3 and complexes **1–6** were measured in the region of 150–4000 cm^{-1}. Characteristic bands confirming the presence of organic ligands in complexes **1–6** were observed in the region of 600–4000 cm^{-1} [45]. The bands were found and assigned as follows: strong bands between 3300 and 3342 cm^{-1} are assignable to $\nu_{(N-H)}$, weak to medium bands between 3092 and 3120 cm^{-1} are assignable to $\nu_{(C-H)ar}$, very strong bands between 1614 and 1623 cm^{-1} may be attributed to $\nu_{(C=N)ar}$ and medium bands between 1163 and 1177 cm^{-1} are assignable to $\nu_{(C-Cl)ar}$. The majority of the bands found between 660 and 900 cm^{-1} can be assigned to skeletal vibrations of a purine moiety of the organic ligands which is present in the complexes studied. Medium to strong bands between 1218 and 1244 cm^{-1} and 1027 and 1033 cm^{-1} attributable to $\nu_{(Car-O)}$, and $\nu_{(C-O)aliph}$, respectively, were found in FT IR spectra of complexes **2**, **3**, **5** and **6**, containing ligands L_2 and L_3. Some new bands appeared in the spectra of the complexes in comparison with free organic ligands in the region between 150 and 600 cm^{-1}. Strong or very strong bands between 340 and 362 cm^{-1} assignable to ν(Pt–Cl) and between 521 and 549 cm^{-1} attributable to $\nu_{(Pt-N)}$ were found [46]. For *cis*-complexes, these bands were splitted into two peaks as compared to *trans*-isomers which clearly supports the *cis*-to-*trans* transformation process in case of the Pt(II) complexes studied.

3.3. Multinuclear NMR studies

Multinuclear NMR study of complexes **1–6** and the ligands L_1–L_3 was performed by means of ^1H, ^{13}C, ^{15}N and ^{195}Pt NMR spectroscopy. Chemical shifts of the selected atoms of the free ligands L_1–L_3 and complexes **1–6**, as found in ^1H and ^{13}C NMR spectra, are given in Table 1, while the ^{15}N NMR and ^{195}Pt NMR spectral data are given in Table 2. Observed signals were assigned and refined by means of ^1H–^1H COSY, ^1H–^{13}C HMQC and ^1H–^{13}C HMBC experiments. The signals found in ^1H and ^{13}C NMR spectra confirmed the presence of organic ligands L_1–L_3 in complexes **1–6** and also proved the coordination of these organic molecules to the central Pt(II) ion. The manner of the ligand L_1–L_3 coordinations to Pt(II) can be deduced from the coordination shifts $\Delta\delta$ ($\Delta\delta = \delta_{complex} - \delta_{ligand}$) as found in both ^1H and ^{13}C NMR spectra of the free ligands and complexes. It is evident from ^1H and ^{13}C spectral data given in Table 1 that the greatest coordination shifts in ^1H NMR spectra were found for the N6H ($\Delta\delta$ = 0.35–0.94 ppm, downfield) and

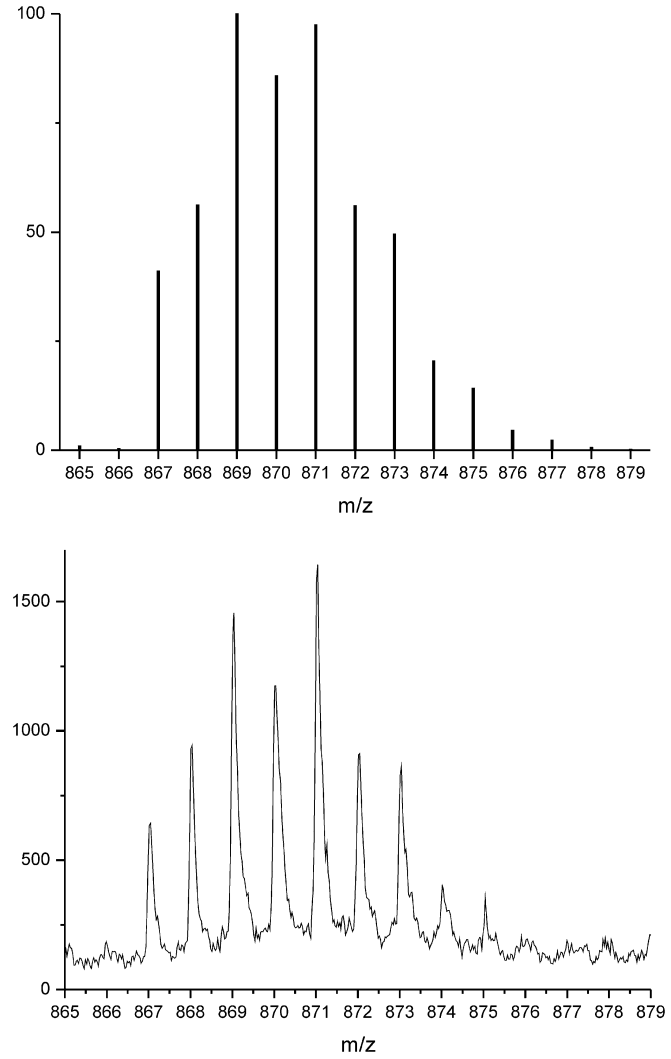

Fig. 2. A representation of the isotopic distribution of the molecular ion of **1** compared to the calculated one obtained using the MASSLYNX software taking into account isotope representation of all the atoms within the molecule.

C8H ($\Delta\delta$ = 0.65–0.97 ppm, downfield) atoms which are situated close to the N7 atom, i.e. to a position where the coordination to platinum(II) [33,34] or palladium(II) [34] can be expected on the basis of our previous findings. These results could be also supported by ^{13}C NMR spectral data, where the greatest chemical shifts were observed for the C5 ($\Delta\delta$ = 3.28–3.69 ppm, upfield) and C8 ($\Delta\delta$ = 2.13–3.33 ppm, downfield) atoms which are adjacent to a coordination site represented by the N7 atom. The signals found in ^{15}N NMR spectra were obtained at natural abundance by long-lasting two dimensional heteronuclear correlation ^{1}H–^{15}N *gs*-HMQC and ^{1}H–^{15}N *gs*-HMBC experiments. Presumable coordination *via* the N7 atom can be also supported by ^{15}N NMR spectral data given in Table 2, from which it is obvious that the greatest coordination shift as compared to the free ligands occurred at the N7 atom ($\Delta\delta$ = 97.67–106.55 ppm, upfield). The chemical shifts of N1, N3, N6 and N9 remained without significant changes, i.e. $\Delta\delta$ were found to be within the interval of 0.80–10.07 ppm that means they are non-significantly influenced by the organic ligand coordinations to platinum. The N7 atom chemical shifts observable in the spectra of the ligands and complexes demonstrably revealed that the coordination of the 6-benzylaminopurine derived ligands to the central platinum(II) ion proceeds *via* the N7 position of the purine moiety.

Generally, it is known, that very important conclusions about the oxidation state of the central Pt ion, stereochemistry, chromophore and isomer types can be obtained from ^{195}Pt NMR experiments, where the significant differences between $\delta(^{195}\text{Pt})$ chemical shifts assignable to *cis* and *trans* complexes are supposed to be observed. It can be evident from the $\delta(^{195}\text{Pt})$ chemical shifts listed in Table 2 that those ones assignable to *cis* isomers **1–3** appeared within the interval of −2017.36 and −2023.06 ppm, while the signals observed for *trans* isomers **4–6** were found between −2061.63 and −2066.07 ppm. The values obtained for complexes **1–3** are in a good agreement with those found for similar complexes of the type *cis*-[Pt(L)$_2$Cl$_2$] (L = methyl derivatives of pyridine), where the $\delta(^{195}\text{Pt})$ values were observed within the interval between −1998 and −2021 ppm [16]. With regard to the fact that we have already studied square-planar platinum(II) complexes bearing 6-benzylaminopurine moiety recently, we can state that the $\delta(^{195}\text{Pt})$ chemical shift values found for *cis*-complexes **1–3** are in good agreement with those determined for Pt(II) complexes of similar structural type and composition published previously [33]. As for *trans*-complexes **4–6**, it is interesting that the observed $\delta(^{195}\text{Pt})$ values between −2061.63 and −2066.07 ppm are shifted to higher fields in comparison with literature data given for similar type of complexes like *trans*-[Pt(L)$_2$Cl$_2$] (L = methyl derivatives of pyridine) being −1948 and −1973 ppm [15]. On the other hand, the achieved values are very close to those published elsewhere, e.g. −2101 ppm for *trans*-[Pt(NH$_3$)$_2$Cl$_2$] [47].

3.3.1. Cis-to-trans isomerization NMR study

It has been known for a long time that square-planar Pt(II) complexes with *cis* arrangement of the type *cis*-[Pt(L)$_2$X$_2$] (where L = NH$_3$ or its derivatives, X = halide) can be transformed into *trans* isomers by re-crystallization from various solvents or by their heating [8–11]. That is why, we decided to prove this ability in the case of the Pt(II) complexes **1–3** involving 6-benzylaminopurine derivatives. A series of 1D (^{1}H, ^{13}C, ^{195}Pt) and 2D (^{15}N *gs*-HMQC and ^{1}H–^{15}N *gs*-HMBC) NMR experiments were per-

Table 1
Selected ^{1}H and ^{13}C NMR spectral data (δ, ppm) for L_1–L_3 and **1–6**

Compound	^{1}H NMR (ppm)				^{13}C NMR (ppm)		
	N6H	C8H	C2	C4	C5	C6	C8
L$_1$	8.67	8.28	153.96	150.57	119.68	156.11	140.04
L$_2$	8.59	8.26	153.96	150.52	119.66	156.01	139.96
L$_3$	8.38	8.29	154.02	150.54	119.75	156.35	140.04
1 *cis*-[Pt(L$_1$)$_2$Cl$_2$]	9.37 (0.70)	9.25 (0.97)	154.23 (0.27)	149.88 (−0.89)	116.37 (−3.31)	155.10 (−1.01)	142.17 (2.13)
2 *cis*-[Pt(L$_2$)$_2$Cl$_2$]	9.29 (0.70)	9.20 (0.94)	154.16 (0.20)	149.84 (−0.68)	116.38 (−3.28)	155.10 (−0.91)	142.17 (2.21)
3 *cis*-[Pt(L$_3$)$_2$Cl$_2$]	9.32 (0.94)	9.15 (0.86)	154.27 (0.25)	149.79 (−0.75)	116.37 (−3.38)	155.12 (−1.23)	142.24 (2.20)
4 *trans*-[Pt(L$_1$)$_2$Cl$_2$]	9.05 (0.38)	8.97 (0.69)	153.91 (−0.05)	149.60 (−0.97)	115.99 (−3.69)	155.15 (−0.96)	143.34 (3.30)
5 *trans*-[Pt(L$_2$)$_2$Cl$_2$]	8.94 (0.35)	8.91 (0.65)	153.85 (−0.11)	149.60 (−0.92)	116.06 (−3.60)	155.28 (−0.73)	143.28 (3.32)
6 *trans*-[Pt(L$_3$)$_2$Cl$_2$]	9.00 (0.62)	9.02 (0.73)	154.13 (0.11)	149.69 (−0.85)	116.11 (−3.64)	155.28 (−1.07)	143.37 (3.33)

Coordination chemical shifts ($\Delta\delta = \delta_{complex} - \delta_{ligand}$) are given in parentheses.

Table 2
Selected ^{15}N NMR spectral data (δ, ppm) for $\mathbf{L_1}$–$\mathbf{L_3}$ and **1**–**6** and ^{195}Pt NMR chemical shifts obtained for **1**–**6**

Compound	N1	N3	N6	N7	N9	^{195}Pt
$\mathbf{L_1}$	227.30	224.00	93.57	239.75	178.70	
$\mathbf{L_2}$	227.32	223.69	95.32	240.15	178.57	
$\mathbf{L_3}$	227.47	223.97	89.27	240.20	178.73	
1 *cis*-$[Pt(L_1)_2Cl_2]$	231.92 (4.62)		99.05 (5.48)	141.62 (−98.13)	184.54 (5.84)	−2017.88
2 *cis*-$[Pt(L_2)_2Cl_2]$	231.10 (3.78)		100.70 (5.38)	141.94 (−98.21)	184.47 (5.90)	−2017.36
3 *cis*-$[Pt(L_3)_2Cl_2]$	231.68 (4.21)		98.32 (9.05)	142.53 (−97.67)	184.50 (5.77)	−2023.06
4 *trans*-$[Pt(L_1)_2Cl_2]$	231.87 (4.57)	224.80 (0.80)	100.10 (6.53)	133.20 (−106.55)	183.83 (5.13)	−2061.63
5 *trans*-$[Pt(L_2)_2Cl_2]$	232.18 (4.86)	224.68 (0.99)	102.52 (7.20)	133.66 (−106.49)	184.19 (5.62)	−2064.02
6 *trans*-$[Pt(L_3)_2Cl_2]$	231.76 (4.29)		99.34 (10.07)	133.98 (−106.22)	184.20 (5.47)	−2066.07

Coordination chemical shifts ($\Delta\delta = \delta_{complex} - \delta_{ligand}$) are given in parentheses.

formed during six months to obtain necessary data for the study of the *cis*-to-*trans* isomerization process in DMF. Although these measurements were performed for all complexes **1–3**, we decided to describe and interpret NMR data regarding the process for complex **1** only because the obtained results were fully comparable for all the studied complexes. Regarding the proper experiment, the sample was measured 20 min after dissolving complex **1** in DMF, and subsequently after one, three and six months. An example of the ^{1}H–^{15}N *gs*-HMBC experiment performed for complex **1** taken one month after the sample dissolution together with its comparison to the spectra of the corresponding free ligand L_1 is presented in Fig. 1A (see Supplementary data). The presence of both *cis* and *trans* isomers (i.e. complexes **1** and **3**) can be clearly seen from the last-mentioned figure. The same conclusion may be drawn from the ^{1}H NMR experiments of complex **1**. The ^{1}H NMR spectra of complex **1**, showing the integral intensities of hydrogen atoms belonging to N6 and C8 atoms measured after 20 min, and 1, 3, and 6 months, as well as proving the presence of both isomers are depicted in Fig. 3. While a trace signal (3%) belonging to the *trans*-isomer can be seen in the spectrum of complex **1** taken 20 min after dissolving of the sample in DMF, after one month, the *cis*-to-*trans* ratio changed approximately to 6:3. Subsequently, the content of *trans* isomer increased gradually and pure *trans* isomer occurred six months after the beginning of the experiment. On the basis of the above described experiments we can state that the *trans* arrangement of the studied complexes is much more stable than the *cis* one in the DMF solutions. Moreover, the performed experiments gave us clear conclusions regarding the time-dependent stability of *cis* complexes **1–3** in DMF and showed us another possibility how to prepare *trans* isomers in a pure form.

In the quest to better describe the solution behavior of *cis*-complexes **1–3**, we were also trying to determine what is occurring with the complexes in a DMF/water mixture. For that reason, complex **1** was dissolved in DMF-d_7:D_2O mixture in 9:1 (v/v) ratio, and we tried to obtain the signals of some hydroxo or aqua species {i.e *cis*-$[Pt(L_n)_2(OH)_2]$ or *cis*-$[Pt(L_n)_2(H_2O)_2]^{2+}$} that were expected to be formed after dissolving the sample in the mentioned solvent mixture. We could not use higher content of water in the mixture due to low solubility of the prepared complexes in water. The sample was measured in time intervals after 20 min, one week, and 1, 3, and 6 months. We used nearly the same experiment formerly in the case of analogous Pd(II) complexes bearing similar types of ligands, where the signals proving the presence of $[Pd(L)_2(OH)_2]$ species were detected [34]. Unfortunately, we were not successful to observe any obvious NMR signals of $(OH)^-$ group in the case of Pt(II)-complexes **1–3**. This might be caused by the fact that the studied Pt(II) complexes are even less soluble than analogous Pd(II) ones in the same solvent mixture used and the complex concentrations were under the detectable limit of the device used. However, the formation of *cis*-$[Pt(L_n)_2(OH)_2]$ or *cis*-$[Pt(L_n)_2(H_2O)_2]^{2+}$ species in the mixture used may be supported by a simple, but very sensitive, analytical experiment. $AgNO_3$ was added to the solution of complex **1** in the DMF/water (9:1) mixture after one week of standing in room temperature. After this time period, a white precipitate originating from AgCl formed and it showed that chlorine anions had to leave the complex in the solvent. To support assumption that organic ligands remain coordinated to platinum, we simultaneously performed additional NMR experiments. It has been found that complex **1** is sufficiently kinetically inert to hold the organic ligands within the inner coordination sphere of platinum, because signals belonging to the uncoordinated ligands were not detected by means of ^{1}H and ^{13}C NMR measurements. It clearly supports conclusion that *cis*-$[Pt(L_n)_2(OH)_2]$ or *cis*-$[Pt(L_n)_2(H_2O)_2]^{2+}$ species are forming in the mixture of solvents used.

3.4. X-ray molecular structures

Crystallographic data and refinement details for complexes **1**, **4** · $(DMF)_2$ and **5** are summarized in Table 3, while the selected bond lengths and angles are given in Table 4. All important hydrogen-bonding interactions were generated by PARST95 [48].

3.4.1. Molecular and crystal structures of *cis*-$[Pt(L_1)_2Cl_2]$ (**1**)

The molecular structure of **1** is shown in Fig. 4 (DIAMOND) [40]. The central Pt(II) ion is coordinated by two chlorido and two L_1 ligands through the N7 atoms of the adenine units forming a *cis*-square-planar coordination around the central atom. The Pt–N and Pt–Cl bond distances are comparable with the average bond lengths of 2.027(4) and 2.291(1) Å, respectively, found in related $PtCl_2N_2$ complexes deposited in the Cambridge Structural Database [49]. Most of atoms of one of two L_1 ligands are disordered over two positions. A degree of the disorder can be seen from different positions of adenine moieties and phenyl rings (see Fig. 4). The adenine moieties are turned in the plane of adenine to each other around the center of rotation lying in the N7A atom about 10.3–13.7°. If Cg1 and Cg2 are defined as the centroids of the first and second disordered phenyl rings, then the Cg1···Cg2 distance is 1.9948(2) Å and the dihedral angle between the rings is 41.8(3)°. Two adenine moieties originating from two L_1 ligands (or three, if we consider the disorder in the case of one L_1 ligand) are almost perpendicular to each other [dihedral angles are 93.6(1)° and 93.4(2)°], and the angle between the platinum coordination plane (i.e. a $PtCl_2N_2$ chromophore) and the purine moiety is 65.13(7)°, 72.80(13)° and 71.99(14)°, respectively. The platinum atom deviates significantly from the planarity of the imidazole ring of the first L_1 ligand [the out-of-plane deviation is 0.2807(3) Å] probably as the result of an intramolecular hydrogen-bonding interactions (N6–H···Cl1: N6···Cl1 = 3.275(5) Å; ∠DHA = 141°; where D = a donor atom, H = the corresponding hydrogen atom, A = an acceptor atom), while the deviations of platinum from the other two disordered imidazole rings are notably lower [0.0636(3) and 0.0745(3) Å].

In the crystal packing, the individual molecules of **1** are connected through strong intermolecular C–H···Cl hydrogen-bonding interactions (C8–H···Cl1: H···Cl1 = 2.65 Å, ∠DHA 171°; 2.54 Å,

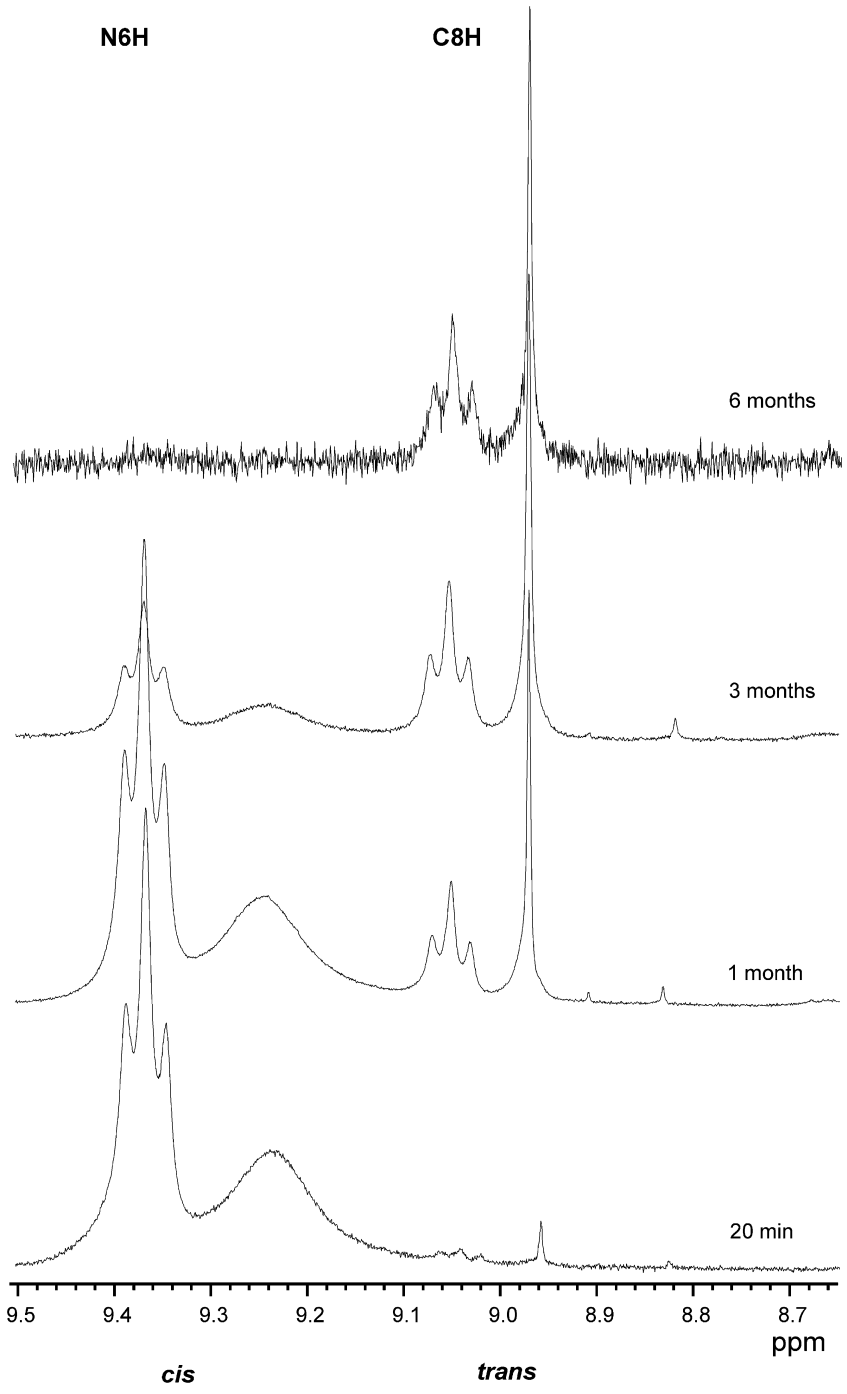

Fig. 3. Selected part of ^{1}H NMR spectra of **1** showing the transformation of *cis* into *trans* isomer of the complex based on the changes of the N6H and C8H signals in dependence on time.

178°; and 2.77 Å; 146°; respectively). The non-bonding intermolecular interactions may be considered to be the main reason of the ligand disorder. Whilst the first position of the disordered L_1 is stabilized by a π interaction [Cl3A···C5: 3.247(8) Å], the second position is stabilized by a π–π stacking interaction [the distance between adjacent parallel imidazole planes is 3.3858 Å].

3.4.2. Molecular and crystal structures of trans-[Pt(L$_1$)$_2$Cl$_2$] (4 · (DMF)$_2$)

The molecular structure of **4** · $(DMF)_2$ (see Fig. 5) revealed a centrosymmetric *trans*-square-planar complex in which the Pt(II) ion is coordinated by two chlorido and two L_1 ligands through the N7 atoms of the adenine moieties [Pt–N: 2.009(2) Å; Pt–Cl: 2.2846(7) Å; N–Pt–Cl: 91.87(7)°]. The Pt(II) ion lies slightly out of the plane of the imidazole ring [the out-of-plane deviation is 0.1332(4) Å]. Similarly to complex **1**, the L_1 ligand is also partially disordered in methyl groups of the isopropyl moiety in the crystal structure of **4** · $(DMF)_2$, i.e. each of the two terminal methyl groups is disordered over two positions. The corresponding methyl groups are turned towards each other about 28° around the axis of rotation lying on the N9–C16 bond. The purine moiety is slightly bent [the dihedral angle between the imidazole and pyrimidine rings is 3.06(13)°] and almost perpendicular to the plane of phenyl group [the dihedral angle is 88.4(1)°].

Table 3
Crystallographic data and refinement for **1**, **4** · $(DMF)_2$ and **5**

	1	**4** · $(DMF)_2$	**5**
Formula	$C_{30}H_{32}Cl_4N_{10}Pt$	$C_{36}H_{46}Cl_4N_{12}O_2Pt$	$C_{32}H_{36}Cl_4N_{10}O_2Pt$
M (g mol^{-1})	869.55	1015.74	929.60
T (K)	110(2)	110(2)	105(2)
λ (Å)	0.71073	0.71073	0.71073
Crystal system	triclinic	monoclinic	monoclinic
Space group	$P\bar{1}$	$P2_1/n$	$P2_1/c$
a (Å)	11.2275(5)	9.2726(8)	8.1507(4)
b (Å)	12.4605(5)	19.8713(16)	15.6503(7)
c (Å)	14.1821(6)	11.0317(11)	14.1585(6)
α (°)	85.638(3)	90	90
β (°)	66.747(4)	96.886(7)	101.086(4)
γ (°)	69.128(4)	90	90
V (Å^3)	1698.46(14)	2018.0(3)	1772.37(14)
Z	2	2	2
D_{calc} (g cm^{-3})	1.700	1.672	1.742
μ (Mo Kα) (mm^{-1})	4.483	3.791	4.306
Crystal size (mm)	0.35 × 0.30 × 0.30	0.35 × 0.10 × 0.10	0.30 × 0.30 × 0.25
Crystal shape and color	yellow prism	orange prism	orange prism
T_{min}/T_{max}	0.82926/1.00000	0.61972/1.00000	0.84874/1.00000
Number data measured	14312	16816	12907
Unique data (R_{int})	5992 (0.0172)	3555 (0.0155)	3126 (0.0164)
Observed data [$I > 2\sigma(I)$]	5313	3175	2576
Final R_1[a], wR_2[b] (observed data)	0.0310, 0.0772[c]	0.0206, 0.0475[d]	0.0251, 0.0626[e]
Final R_1[a], wR_2[b] (all data)	0.0375, 0.0800[c]	0.0245, 0.0493[d]	0.0358, 0.0689[e]
ρ_{max}, ρ_{min} (e Å^{-3})	2.282, −1.813	0.710, −0.295	0.694, −0.586

Where [a] $R = \sum(|F_o| - |F_c|)/\sum|F_o|$, [b] $wR_2 = [\sum w(|F_o| - |F_c|)^2/\sum(F_o)^2]^{1/2}$, [c] $w = 1/[\sigma^2(F_o) + (0.0375P)^2 + 10P]$, [d] $w = 1/[\sigma^2(F_o) + (0.015P)^2 + 10P]$, [e] $w = 1/[\sigma^2(F_o) + (0.025P)^2 + 10P]$ and $P = (F_o^2 + 2F_c^2)/3$.

Table 4
Selected bond lengths (Å) and angles (°) for **1**, **4** · $(DMF)_2$ and **5**

	1	**4** · $(DMF)_2$	**5**
Bond lengths			
Pt(1)–N(7)	2.032(4)	2.009(2)	2.008(4)
Pt(1)–N(7A)	2.022(4)	2.009(2)	2.008(4)
Pt(1)–Cl(1)	2.2873(14)	2.2846(7)	
Pt(1)–Cl(1A)		2.2846(7)	
Pt(1)–Cl(2)	2.2834(13)		2.2954(11)
Bond angles			
N(7)–Pt(1)–Cl(2)	178.63(12)		91.02(11)
N(7)–Pt(1)–Cl(1A)		88.13(7)	
N(7A)–Pt(1)–N(7)	89.74(16)	180.0	180.0
N(7A)–Pt(1)–Cl(1A)		91.87(7)	
N(7A)–Pt(1)–Cl(2)	88.98(12)		88.98(11)
N(7A)–Pt(1)–Cl(1)	179.17(13)	88.13(7)	
N(7)–Pt(1)–Cl(1)	90.04(12)	91.87(7)	
Cl(2)–Pt(1)–Cl(1)	91.25(5)		
Cl(1A)–Pt(1)–Cl(1)		180.0	
Cl(2)–Pt(1)–Cl(2A)			180.0

Symmetry transformations used to generate equivalent atoms labelled A for **4** · $(DMF)_2$: $-x+1, -y+1, -z+1$; for **5**: $-x+1, -y+1, -z+1$.

The crystal packing of **4** · $(DMF)_2$ is stabilized by hydrogen-bonding interactions involving chlorine and some atoms of DMF (e.g. C8–H···O1: H···O1 = 2.16 Å; ∠DHA = 176°; C20–H20C···Cl1: H···Cl1 = 2.78 Å; ∠DHA = 155°; C20–H20A···Cl1: H···Cl1 = 2.81 Å; ∠DHA 148°) forming infinite linear complex–$(DMF)_2$–complex chains.

3.4.3. Molecular and crystal structures of trans-$[Pt(L_2)_2Cl_2]$ (**5**)

The central part of the molecular structure of **5** (see Fig. 6) is very similar to that of **4** · $(DMF)_2$. The complex is centrosymmetric

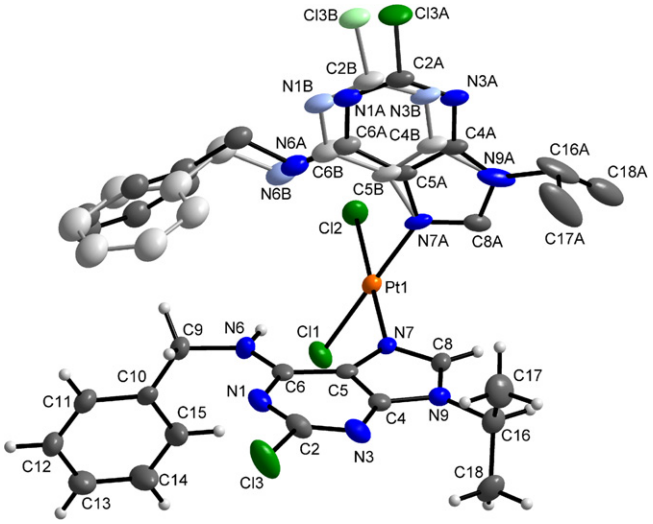

Fig. 4. Molecular structure of complex **1**, showing the atom numbering scheme. Thermal ellipsoids are drawn at the 40% probability level. Some of atoms are disordered over two positions. Some of H-atoms were omitted for clarity.

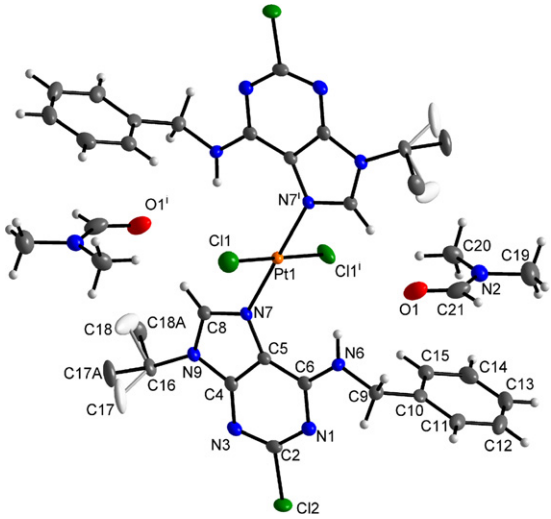

Fig. 5. Molecular structure of the centrosymmetric complex **4** · $(DMF)_2$, showing the atom numbering scheme [symmetry code: (i) $1-x, 1-y, 1-z$]. Some of atoms are disordered over two positions. H-atoms belonging to the disordered part of the molecule were omitted for clarity.

with a *trans*-square-planar coordination around the central Pt(II) ion which is coordinated by two chlorido and two L_2 ligands via the N7 atoms [Pt–N: 2.008(4) Å; Pt–Cl: 2.2954(11) Å; N–Pt–Cl: 91.02(11)°]. The platinum(II) ion lies significantly out of the plane of the imidazole ring [the deviation is 0.1956(1) Å]. The isopropyl group and chlorine atom of the L_2 ligand is disordered over two positions. Atoms of the isopropyl group are turned towards each other around the N9–C16 rotation axis about 31.891(2)°. The purine moiety is also slightly bent [the dihedral angle between the imidazole and pyrimidine rings is 5.23(2)°]. The main structural differences between **4** · $(DMF)_2$ and **5** are in intra- and intermolecular interactions. While the interactions in the crystal structure of **4** · $(DMF)_2$ are affected by the presence of DMF molecules, their absence in **5** result in a more compact molecular packing. The phenyl group of one L_2 ligand in **5** is stabilized by π-interactions with the purine of the other L_2 ligand [if Cg1 is the centroid of the phenyl ring of the first L_2, H8···Cg1 distance is 3.07 Å, H8 distance from

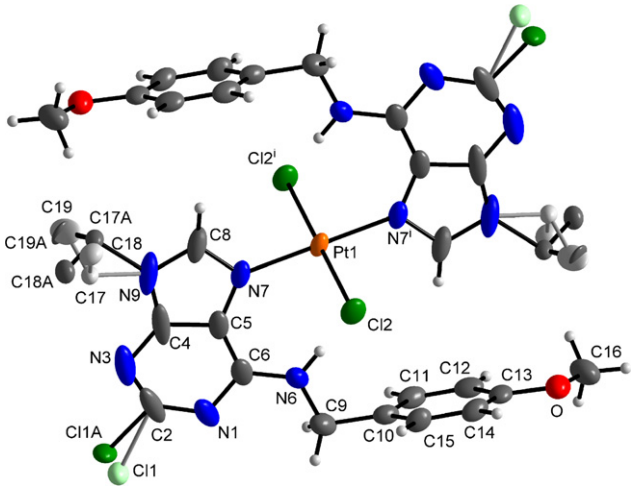

Fig. 6. Molecular structure of the centrosymmetric complex **5**, showing the atom numbering scheme [symmetry code: (i) $1-x, 1-y, 1-z$]. Thermal ellipsoids are drawn at the 50% probability level. Some of atoms are disordered over two positions. H-atoms belonging to the disordered part of the molecule were omitted for clarity.

the plane of the phenyl ring is 3.04 Å, and the dihedral angle between the purine and phenyl moieties is 77.35(13)°]. The crystal packing is further stabilized by intramolecular hydrogen bonds N6–H···Cl2 [N6···Cl2 = 3.281(5) Å; ∠DHA = 139°] and intermolecular Cl···N π–π interactions [Cl2···N1: 3.289(6) Å] arranging molecules of **5** into infinite linear chains.

3.4.4. Crystal structure summary

Generally, the Pt–N and Pt–Cl bond distances in complexes **1**, **4** · $(DMF)_2$ and **5** are in the range of 2.008–2.032 Å, and 2.2834–2.2954 Å, respectively. They are quite comparable to those found for the *trans*-$[PtCl_2(L)_2]$ complex involving two coordinated 2-chloro-6-[(3-hydroxybenzyl)amino]-9-isopropylpurine ligands (L) [50] and also to the average bond lengths found for the Pt–N and Pt–Cl bond lengths (2.02, and 2.29 Å, respectively) in related $PtCl_2N_2$ complexes as reported in the Cambridge Structural Database [49]. In all the discussed complexes, the central platinum atom deviates significantly from the planarity of purine moieties. The degree of deformation of organic ligands within the complexes is markedly influenced by non-bonding intramolecular and intermolecular interactions.

3.5. Biological activity

Complexes **1–6** were screened for their cytotoxic effects *in vitro* against four human cancer cell lines: MCF7, G361, K562 and HOS. Based on the fact that the prepared complexes **1–6** were only slightly soluble in water, and the testing procedure necessarily uses water as a medium, we were limited by the solubility of the complexes in water. That is why we could only prepare water solutions with the complex concentrations being maximally 5 μM. At higher concentrations, the complexes precipitated from the water medium. Unfortunately, the complexes showed to be non-cytotoxic within this low concentration range.

4. Conclusions

We have prepared and fully characterized six new *cis* and *trans* square-planar Pt(II) complexes involving derivatives of plant growth hormones, called cytokinins, derived from 6-benzylaminopurine moiety, and having a general formula of $[Pt(L_n)_2Cl_2]$. X-ray molecular structures of the complexes *cis*-$[Pt(L_1)_2Cl_2]$ (**1**), *trans*-$[Pt(L_1)_2Cl_2]$ (**4** · $(DMF)_2$), and *trans*-$[Pt(L_2)_2Cl_2]$ (**5**) have been determined and supported the composition and stereochemistry following from other physical techniques used for the characterization of the complexes. Moreover, the dynamic *cis*-to-*trans* isomerization process in DMF solutions, as well as the behavior of the complexes in a DMF/water solution has been investigated by the means of multinuclear NMR spectroscopy. The obtained results elucidated and extended our knowledge about time-dependent solution behavior of these complexes. All the complexes were tested *in vitro* against four human cancer cell lines (MCF7, G361, K562 and HOS). The tested compounds could only be tested at low concentrations (up to 5 μM) because of their low solubility in water which is a necessary medium in the testing procedure used. Unfortunately, at this concentration, the complexes, as well as the initial free ligands, showed no cytotoxicity.

Acknowledgements

This work was funded by The Ministry of Education, Youth and Sports of the Czech Republic (a Grant No. MSM6198959218). The authors thank to Assoc. Prof. Marek Šebela, PhD for performing of MALDI-TOF experiments and Ms. Olga Hustáková for her help with biological testing.

Appendix A. Supplementary data

CCDC 683645, 683646 and 683647 contain the supplementary crystallographic data for **1**, **4** · $(DMF)_2$, and **5**. These data can be obtained free of charge via http://www.ccdc.cam.ac.uk/conts/retrieving.html, or from the Cambridge Crystallographic Data Centre, 12 Union Road, Cambridge CB2 1EZ, UK; fax: (+44) 1223-336-033; or e-mail: deposit@ccdc.cam.ac.uk. Supplementary data associated with this article can be found, in the online version, at doi:10.1016/j.poly.2008.05.021.

References

[1] B. Rosenberg, L. Van Camp, T. Krigas, Nature 205 (1965) 698.
[2] E. Wong, Ch.M. Giandomenico, Chem. Rev. 99 (1999) 2451.
[3] R.R. Barefoot, J. Chromatogr. B 751 (2001) 205.
[4] Ch.X. Zhang, S.J. Lippard, Curr. Opin. Chem. Biol. 7 (2003) 481.
[5] L.R. Kelland, S.Y. Sharp, C.F. O'Neill, F.I. Raynaud, P.J. Beale, I.R. Judson, J. Inorg. Biochem. 77 (1999) 111.
[6] Y. Najarjeh, J.M. Perez, C. Navarro-Ranninger, D. Gibson, J. Med. Chem. 45 (2002) 5189.
[7] Y.N. Kukushkin, Platinum Met. Rev. 35 (1991) 28.
[8] P.C. Kong, F.D. Rochon, Inorg. Chim. Acta 61 (1982) 269.
[9] C.J.L. Lock, M. Zvagulis, Inorg. Chem. 20 (1981) 1817.
[10] C.J.L. Lock, M. Zvagulis, Acta Crystallogr., Sect. B 36 (1980) 2140.
[11] J.P. Bradford, R. Faggiani, C.J.L. Lock, Acta Crystallogr., Sect. B 37 (1981) 243.
[12] P.C. Kong, F.D. Rochon, Can. J. Chem. 57 (1979) 526.
[13] P.C. Kong, F.D. Rochon, Can. J. Chem. 59 (1981) 3293.
[14] V.Y. Kukushkin, D. Tudela, Y.A. Izotova, V.K. Belsky, A.I. Stash, Polyhedron 17 (1998) 2455.
[15] Ch. Tessier, F.D. Rochon, Inorg. Chim. Acta 322 (2001) 37.
[16] F.D. Rochon, V. Buculei, Inorg. Chim. Acta 357 (2004) 2218.
[17] K.R. Koch, Y. Wang, A. Coetzee, J. Chem. Soc., Dalton Trans. (1999) 1013.
[18] J. Reedijk, PNAS 100 (2003) 3611.
[19] O. Nováková, J. Kašpárková, J. Malina, G. Natile, V. Brabec, Nucleic Acids Res. 31 (2003) 6450.
[20] G. McGowan, S. Pearsons, P.J. Sadler, Inorg. Chem. 44 (2005) 7459.
[21] J. Vinje, E. Sletten, AntiCancer Agents Med. Chem. 7 (2007) 35.
[22] D.S. Letham, New Zeal. J. Bot. 1 (1964) 336.
[23] C.O. Miller, F. Skoog, M.H. Von Saltza, F.M. Strong, J. Am. Chem. Soc. 77 (5) (1955) 1392.
[24] F. Skoog, H.Q. Hamzi, A.M. Szweykowska, N.J. Leonard, K.L. Carraway, T. Fujii, J.P. Helgeson, R.N. Leoppky, Phytochemistry 6 (9) (1967) 1169.
[25] P.J. Davies, Plant Hormones. Biosynthesis, Signal Transduction, Action, Kluwer Academic Publishers, Dordrecht, The Netherlands, 2004.
[26] S. Gan, R.M. Amasino, Science 270 (1995) 1986.

[27] G. Haberer, J.J. Kieber, Plant Physiol. 128 (2002) 354.
[28] M. Legraverend, P. Tunnah, M. Noble, P. Ducrot, O. Ludwig, D.S. Grierson, M. Leost, L. Meijer, J. Endicott, J. Med. Chem. 43 (2000) 1282.
[29] M.J. Moon, S.K. Lee, J.W. Lee, W.K. Song, S. W Kim, J.I. Kim, C. Cho, S.J. Choi, Y.C. Kim, Bioorg. Med. Chem. 14 (2006) 237.
[30] R.M. Goldsteyn, Cancer Lett. 217 (2005) 129.
[31] W.F. DeAzevedo, S. Leclerc, L. Meijer, L. Havlíček, M. Strnad, S.H. Kim, Eur. J. Biochem. 243 (1997) 518.
[32] F.I. Raynaud, S.R. Whittaker, P.M. Fisher, S. McClue, M.I. Walton, S.E. Barrie, M.D. Garrett, P. Rogers, S.J. Clarke, L.R. Kelland, M. Valenti, L. Brunton, S. Eccles, D.P. Lane, P. Workman, Clin. Cancer Res. 11 (13) (2005) 4875.
[33] L. Szüčová, Z. Trávníček, M. Zatloukal, I. Popa, Bioorg. Med. Chem. 14 (2006) 479.
[34] Z. Trávníček, L. Szüčová, I. Popa, J. Inorg. Biochem. 101 (2007) 477.
[35] M. Maloň, Z. Trávníček, M. Maryško, J. Marek, K. Doležal, J. Rolčík, M. Strnad, Transition Met. Chem. 27 (2002) 580.
[36] Z. Trávníček, V. Kryštof, M. Šipl, J. Inorg. Biochem. 100 (2006) 214.
[37] A. Klanicová, Z. Trávníček, I. Popa, M. Čajan, K. Doležal, Polyhedron 25 (2006) 1421.
[38] CRYSALIS RED and CRYSALIS CCD, Version 1.171.23, Oxford Diffraction Ltd., Abingdon, England, 2006.
[39] G.M. Sheldrick, Acta Crystallogr., Sect. A 46 (1990) 467.
[40] K. Brandenburg, DIAMOND (Release 3.1e), Grystal Impact GbR, Bonn, Germany, 2006.
[41] P.C. Kong, F.D. Rochon, Inorg. Chim. Acta 83 (1984) 65.
[42] W.J. Geary, Coord. Chem. Rev. 7 (1971) 81.
[43] MASSLYNXTM, version 4.0, Waters, Milford, MA, USA, 2005.
[44] W. Henderson, J.S. McIndoe, Mass Spectrometry of Inorganic and Organometallic Compounds, John Wiley & Sons, Ltd., Chichester, England, 2005.
[45] C.J. Pouchert, The Aldrich Library of Infrared Spectra, Aldrich Chemical Company Press, Milwaukee, USA, 1981.
[46] K. Nakamoto, Infrared and Raman Spectra of Inorganic and Coordination Compounds. Part B: Applications in Coordination, Organometallic and Bioinorganic Chemistry, John Wiley & Sons Ltd., New York, England, 1991.
[47] F.H. Appleton, F.J. Pesch, M. Wienken, S. Menzer, B. Lippert, Inorg. Chem. 31 (1992) 4410.
[48] M. Nardelli, J. Appl. Crystallogr. 28 (1995) 659.
[49] F.H. Allen, Acta Crystallogr., Sect. B 58 (2002) 380.
[50] Z. Trávníček, J. Marek, L. Szüčová, Acta Crystallogr., Sect. E 62 (2006) m1 482.